

# 2221. Dynamic analyses of osteoblast vibrational responses: a finite element viscoelastic model

Liping Wang<sup>1</sup>, Cory J. Xian<sup>2</sup>

<sup>1,2</sup>The Third Affiliated Hospital of Southern Medical University, Orthopaedic Hospital of Guangdong Province, Guangzhou, 510630, China

<sup>1,2</sup>Sansom Institute for Health Research, School of Pharmacy and Medical Sciences, University of South Australia, Adelaide, SA 5001, Australia

<sup>2</sup>Corresponding author

**E-mail:** <sup>1</sup>[liping.wang@mymail.unisa.edu.au](mailto:liping.wang@mymail.unisa.edu.au), <sup>2</sup>[cory.xian@unisa.edu.au](mailto:cory.xian@unisa.edu.au)

Received 28 May 2016; received in revised form 8 July 2016; accepted 18 July 2016

DOI <https://doi.org/10.21595/jve.2016.17211>

**Abstract.** Mechanotransduction is an important process that influences bone remodeling and maintains viability of bone cells. To understand the effect of the vibrational mechanical stimulation on biomechanic responses of bone cells, a viscoelastic osteoblast finite element (FE) model was developed. Firstly, the mode shapes and natural frequencies of a spreading osteoblast were assessed using the FE modal analysis. The osteoblast FE model predicted the natural frequencies of osteoblasts (within the range about 19.99-34.48 Hz). Then, the effect of acceleration on the vibrational responses of in-vitro cultured osteoblasts was investigated. Three different accelerations of base excitation were selected (0.15 *g*, 0.3 *g* and 0.5 *g*, where  $g = 9.8 \text{ m/s}^2$ ) and the vibrational responses (displacement, strain and stress) of osteoblasts were simulated. It was found that values of displacement, strain and stress increase with the increase of base excitation acceleration. In addition, the response values in *Z*-direction are much higher than those in the other directions (*X*, *Y*-direction) for the same base excitation acceleration. These findings will provide useful information to understand how vibrational mechanical stimulus influences bone cells and provide guidance for in vitro cell culture and experimental research and ultimately clinical treatment using the external vibrating loading.

**Keywords:** vibration modes, natural frequency, modal analysis, finite element analysis, osteoblast.

## 1. Introduction

Mechanical stimuli always act on living cells of the human in whole life [1]. It is widely known that bone is a dynamic tissue, because the mechanical stimulus can control the bone resorption and/or apposition activities the bone remodelling cells and thus modify bone mass, shape and/or strength [2-5]. Since 1970 [6], many forms of mechanical stimuli have been used to analyse the biomechanic responses of bone cells in vitro, e.g. fluid shear stress [7], strain [8] and vibration [9]. While cells are complex systems, to investigate biological responses of cells under external mechanical stimuli, cells can be modelled as some simple models, e.g. linear elastic models [8, 10], viscoelastic models [11, 12], power-law structural damping model [13, 14], biphasic models [15, 16] and the tensegrity model [17, 18].

Finite element (FE) analysis is a very powerful and efficient research tool to simulate the responses of cells under the external dynamic mechanical stimuli [8, 19-21]. With the development of commercial FE analysis software, now it is possible to simulate the three-dimensional (3D) structure of cells. Shin and Athanasiou simulated the biphasic mechanical parameters of osteoblasts-like cells using the FE method [15]. McGarry and Prendergast developed a 3D FE model of an adherent eukaryote cell [22]. Katzung et al. simulated the large deformation behaviour for the maturing adipocytes using a 3D FE model [23]. To simulate the cellular mechanics behaviours like large deformation, the 3D cell-specific FE model was developed based on confocal microscopy [24]. In a recent study, to investigate viscoelastic property of bone cells under fluid flow, a new method was used combining fluid-structure interaction FE model and quasi-3D microscopy [12].

Some previous studies have obtained good achievements in studying viscoelastic material properties of bone cells. For examples, elastic and viscoelastic tests were used to measure the biomechanical properties of individual cells (including spreading osteoblasts) using anatomic force microscope [25], and the viscoelastic material property of single adherent bone cells (osteocytes) was investigated by using a new non-invasive approach [12]. Furthermore, vibration analyses of the spreading bone cells (osteoblasts) were conducted using linear elastic FE continuum and tensegrity models to investigate vibrational characteristics of bone cells [26, 27]. However, the viscoelastic property was ignored in these studies [26, 27]. Since, it is well accepted that the viscoelastic property of cells play an important role in many biological and biophysical processes and responses [28-30], it is necessary to analyse the processes and mechanisms of vibrational responses of bone cells using the viscoelastic model.

In the current study, we aimed to analyse the biomechanical responses of osteoblasts to the external vibrational stimuli using a 3D FE viscoelastic model of osteoblasts. The main goals of this study were (1) to create the idealized continuum 3D FE models of osteoblasts; (2) to obtain natural frequencies and mode shapes of osteoblasts using the FE model; (3) to investigate the harmonic responses (like resonance frequency, displacement, strain and stress) to the different base excitation acceleration (i.e. 0.15g, 0.3g and 0.5g) of the osteoblast FE model.

## 2. Materials and methods

### 2.1. Model geometry and FE modelling

Based on the experimental investigation [31] and analytical model [22], the shape and geometry of an osteoblast are shown in Fig. 1. The osteoblast is comprised of three components, i.e. cell membrane, cytoplasm and nucleus. The idealized geometry of the osteoblast is a part of the sphere. The nucleus was always modelled as a sphere [32] or ellipsoid [22, 26, 27], and the shape of the nucleus was modelled as an ellipsoid in this study. Based on the investigation of McGarry and Prendergast [22], the volumes of the nucleus and whole cell were estimated as about 105  $\mu\text{m}^3$  and 3000  $\mu\text{m}^3$ , respectively. Normally, the cell thickness was about 0.1-0.5  $\mu\text{m}$  [32], and in this study the cell membrane was modelled as a shell with the thickness being about 6 nm [33, 34]. The cell height was about 2-20  $\mu\text{m}$  [22, 34-36]. For an idealized model, the bottom surface of the cell can be an ellipse [26, 27, 37] or a circle [22, 35, 36, 38]. In this study, the microfilament and the microtubules were ignored. The dimensions of this model are given in Table 1.

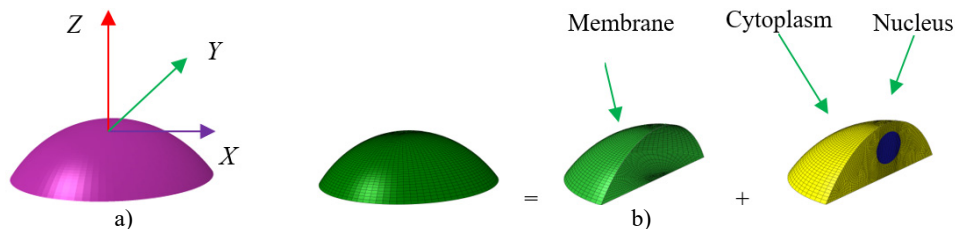


**Fig. 1.** Geometry and an idealized 3D finite element (FE) model of an osteoblast: a) geometry and b) whole FE modelling

**Table 1.** Geometry property and element data for the osteoblast finite element modelling

Dimension					Number of elements		
Cell height ( $\mu\text{m}$ )	Surface ( $\mu\text{m}^2$ )	Bottom area ( $\mu\text{m}^2$ )	Volume ( $\mu\text{m}^3$ )	Nucleus volume ( $\mu\text{m}^3$ )	Nucleus	Cytoplasm	Membrane
8.03	891.97	696.53	3010.90	104.72	23424	111808	10048

In this study, according to the corresponding geometry of the osteoblast, an idealized 3D FE model was developed (Fig. 1). ABAQUS 6.14 (SIMULIA, Providence, RI) was used to implement

the FE analysis for the simulations. For the FE model, eight-node hexahedral elements (C3D8R for reducing the run time) were selected for the solid regions (including nucleus and cytoplasm). In addition, the cell membrane was meshed as the shell element S4R to save the run time. The FE element numbers of the nucleus, cytoplasm and membrane are presented in Table 1. To ensure a no-slip behaviour between nucleus-cytoplasm and cytoplasm-cell membrane, the tie constraint was used in this study.

## 2.2. Materials

In this study, cell membrane and the nucleus were assumed as the linear isotropic elastic materials and cytoplasm was assumed as the linear viscoelastic material. The standard linear solid viscoelastic model (Zener model) can be described as Fig. 2.

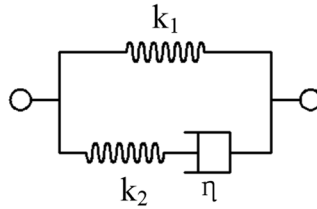


Fig. 2. A standard linear solid viscoelastic model

The extensional relaxation function is described [39]:

$$E_R(t) = k_1 + k_2 e^{-t/\tau_R}, \quad \tau_R = \frac{\eta}{k_2}, \quad (1)$$

where  $\eta$  is the damping coefficient (viscosity);  $k_1$  and  $k_2$  are spring stiffnesses (constants).

When  $t = 0$  and  $t \rightarrow \infty$ , based on Eq. (1), the extensional relaxation function may be written as Eq. (2), respectively:

$$E_R(t = 0) = E_0 = k_1 + k_2, \quad E_R(t \rightarrow \infty) = E_\infty = k_1, \quad (2)$$

where  $E_0$  and  $E_\infty$  are the instantaneous modulus and equilibrium modulus, respectively.

Based on Eq. (1b) and Eq. (2), the following equations can be obtained:

$$k_2 = E_\infty \frac{\tau_\sigma - \tau_R}{\tau_R}, \quad \eta = E_\infty (\tau_\sigma - \tau_R), \quad \tau_\sigma = \frac{\eta}{k_1 k_2} (k_1 + k_2). \quad (3)$$

Normally, the prony series is applied to simulate the linear viscoelastic behaviour of bone cells including osteoblasts. The prony series can be expressed as [39]:

$$G_R(t) = G_0 \left[ 1 - \sum_{i=1}^N g_i (1 - e^{-t/\tau_i}) \right], \quad G_0 = \frac{3K(k_1 + k_2)}{9K - (k_1 + k_2)}, \quad (4)$$

where,  $G_0$  is the instantaneous shear and bulk moduli (when  $t = 0$ );  $G_R(t)$  is the time-dependent shear relaxation modulus;  $g_i$  and  $\tau_i$  are the shear weighing factor (normally ranged between 0 and 1) and the relaxation time constant, respectively.

Based on the study of Qiu et al. [12], the viscoelastic parameters of the bone cell,  $E_0$ ,  $E_\infty$ , and  $\eta$  were selected as  $0.49 \pm 0.11$  kPa,  $0.31 \pm 0.044$  kPa and  $4.07 \pm 1.23$  kPa, respectively. The elastic modulus of the membrane of the adherent eukaryotic cell was selected as 1 kPa [22, 40]. Young modulus ratio of cytoplasm and nucleus was chosen at 1:4 [22, 27, 41]. Moreover, Poisson's ratios for membrane, cytoplasm and nucleus were assumed 0.3, 0.37 and 0.37, respectively in this study.

The initial density of the cell was assumed as 1250 kg/m<sup>3</sup> which was used as the density of cytoplasm [42], and the density ratio was assumed 0.4:1:1.2 to membrane, cytoplasm and nucleus [40]. Thus in this study, the densities of membrane, cytoplasm and nucleus of the osteoblast are 500 kg/m<sup>3</sup>, 1250 kg/m<sup>3</sup> and 1500 kg/m<sup>3</sup>, respectively. The detailed material properties for the FE model are given in Table 2.

**Table 2.** Material properties of the osteoblast finite element model

Material properties		
Membrane	Cytoplasm	Nucleus
$E_0 = 1.0 \text{ kPa}, \nu = 0.3, \rho = 500 \text{ kg/m}^3$	$E_0 = 0.49 \text{ kPa}, E_\infty = 0.31 \text{ kPa}, \eta = 4.07 \text{ kPa s}, \nu = 0.37 \text{ and } \rho = 1250 \text{ kg/m}^3$	$E_0 = 1.96 \text{ kPa}, \nu = 0.37, \rho = 1500 \text{ kg/m}^3$

### 2.3. Modal analysis

Modal analysis was used to find out the natural frequencies of the bone cell. Natural frequency extraction is an eigenvalue analysis procedure, which determines the natural frequencies and shapes of mode for a structure. In this study, software ABAQUS was used to conduct the natural frequency extraction. The governing dynamic equation of the response in ABAQUS can be expressed as [39] follows:

$$M\ddot{u} + C\dot{u} + Ku = P, \quad u = \phi \sin(\omega t) \text{ or } \phi e^{i\omega t}, \quad P = \bar{P} \cos(\omega t), \quad (5)$$

where  $M$ ,  $C$  and  $K$  (symmetric and positive definite) are the mass matrix, damping coefficient matrix and spring stiffness matrix in the system, respectively.  $P$  is harmonic loading;  $\phi$  is the eigenvector;  $\omega$  is the circular frequency; and  $\ddot{u}$ ,  $\dot{u}$  and  $u$  are the acceleration vector, velocity vector and displacement vector, respectively.

In this study, the vibration of the system with only one degree-of-freedom was considered. To investigate the effect of acceleration on the cell, the different accelerations of base excitation were used in the simulation, i.e. 0.15g, 0.3g and 0.5g, respectively. It is well known that acceleration ( $g$  forces,  $g = 9.8 \text{ m/s}^2$ ) is the one of the best terms to describe vibration intensity, such as low intensity if the value of acceleration  $< 1g$  and high intensity if the value of acceleration  $\geq 1g$  [43, 44]. In the simulation, zero displacement was applied at the bottom surface of the cell model. That means three translational directions of bottom surface of FE model were constrained.

## 3. Results

### 3.1. Natural frequency extraction

The natural frequency (vibration resonant frequencies) and vibration mode shape of the FE model were obtained. The first ten natural frequencies are given in Table 3 and mode shapes of the first ten modes are presented in Fig. 3. To validate these results, the natural frequency from one previous study [27] is presented in Table 3 as well. Only the first five natural frequencies were given in the reference [27] and the frequency range was between 18.11 and 21.05 Hz. In addition, the range of the natural frequency was reported between 9.95-211.05 Hz for a spreading bone cell [26]. It can be seen that the varying trend and natural frequency values of the current study are in accordance with those of the previous study [26, 27].

**Table 3.** Natural frequencies of the first ten modes of the finite element model (FEM) of an osteoblast

	1st	2nd	3rd	4th	5th	6th	7th	8th	9th	10th
FEM	19.99	20.01	24.09	30.12	30.15	30.48	31.97	31.98	34.43	34.48
Reference [27]	18.11	18.13	19.31	20.87	21.05					
Difference %	9.40	9.40	19.84	30.71	30.18					

From Fig. 3, it can be observed that the 1st and 2nd modes presented one direction oscillation, the 3rd and 6th modes showed the torsional modes, the 4th and 5th modes presented four oscillations, the 7th and 8th modes showed three oscillations, and the 9th and 10th modes showed two oscillations. These suggest that the shape and material properties of the bone cell may affect the natural frequency.

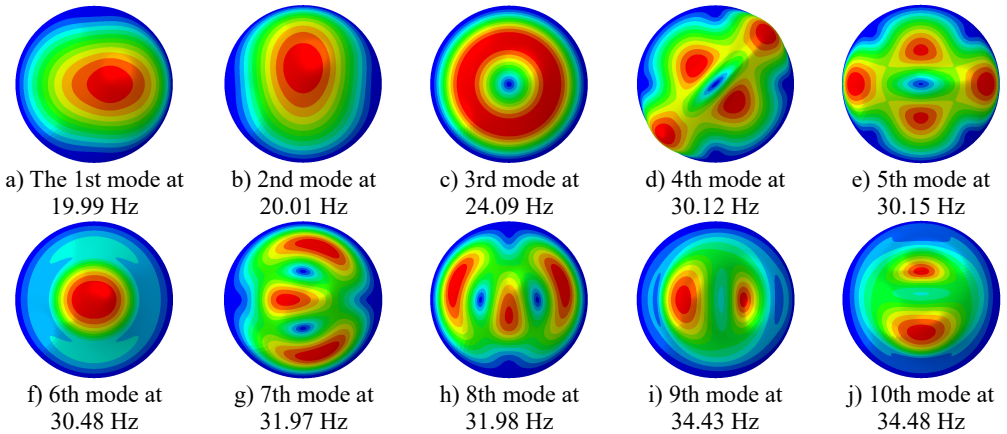


**Fig. 3.** Mode shapes of the first ten vibration modes

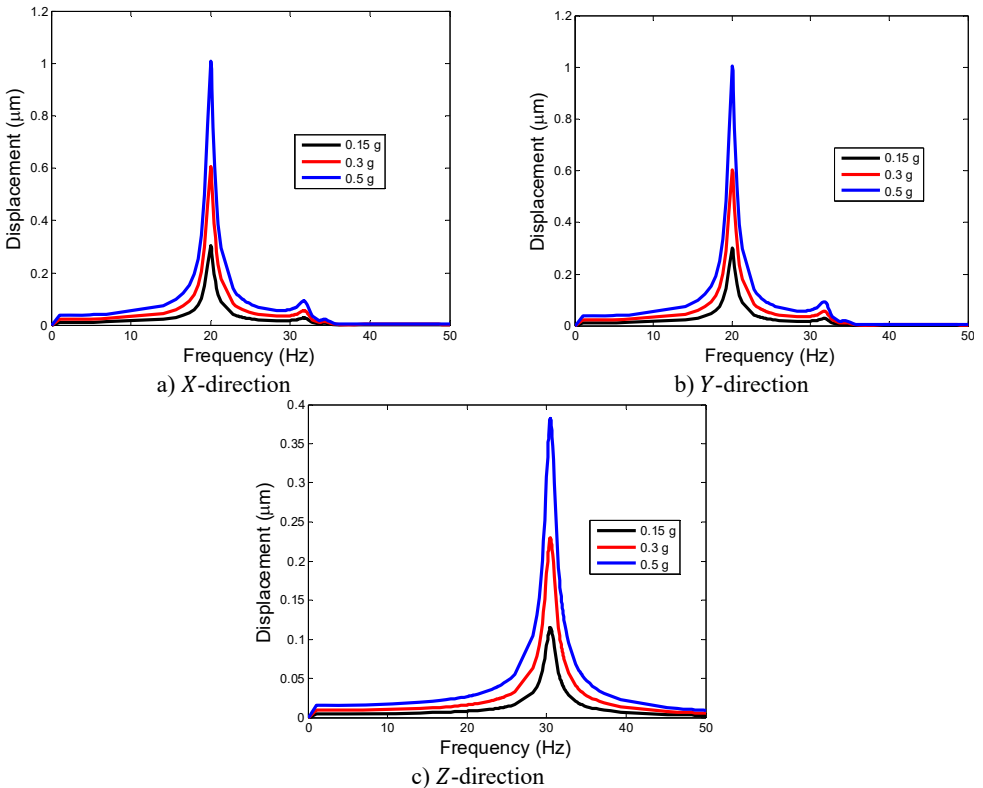


**Fig. 4.** The displacement of the centre of nucleus versus frequency

### 3.2. Harmonic vibration

As shown in Table 3, the lowest and highest natural frequencies are about 20 Hz and 34.48 Hz,

respectively. Based on the natural frequencies and the assumed uniform acceleration of base excitation with the frequency range between 1 and 50 Hz, the harmonic responses of the viscoelastic FE model were computed for three different acceleration values, i.e.  $0.15g$ ,  $0.3g$  and  $0.5g$ . The responses of displacement, strain and stress at the centre of the nucleus in the different directions ( $X$ ,  $Y$ ,  $Z$ -directions) to the harmonic vibration were investigated.

The displacement responses at the centre of nucleus are plotted as Fig. 4 for the different acceleration values of  $0.15g$ ,  $0.3g$  and  $0.5g$  and the different directions ( $X$ ,  $Y$ ,  $Z$ -directions). The mode shapes of the viscoelastic FE models under the  $0.3g$  base excitation at different frequencies ( $0$ ,  $6.937$ ,  $20.00$ ,  $30.01$ ,  $39.33$  and  $50$  Hz) in  $X$ -direction,  $Y$ -direction and  $Z$ -direction are presented in Fig. 5.

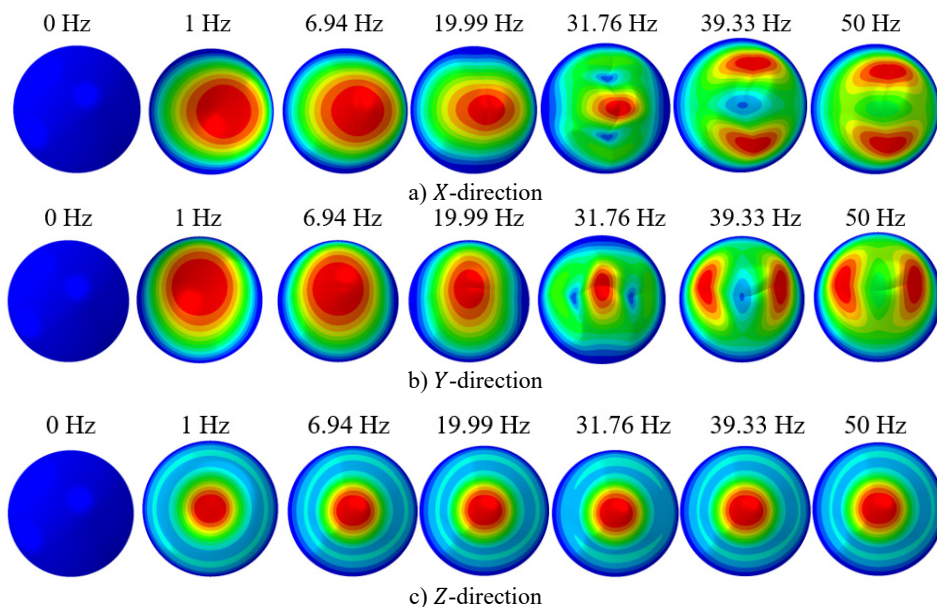


**Fig. 5.** Mode shapes at the different frequencies under the  $0.3g$  acceleration

The strain responses at the centre of nucleus are plotted as Fig. 6 for the different acceleration values ( $0.15g$ ,  $0.3g$  and  $0.5g$ ) and in the different directions ( $X$ ,  $Y$ ,  $Z$ -directions). The strain distributions of the FE models under the  $0.3g$  base excitation at different frequencies ( $0$ ,  $6.937$ ,  $20.00$ ,  $30.01$ ,  $39.33$  and  $50$  Hz) in  $X$ -direction,  $Y$ -direction and  $Z$ -direction were also presented as Fig. 7.

The stress responses at the centre of nucleus are plotted as Fig. 8 for the different acceleration values ( $0.15g$ ,  $0.3g$  and  $0.5g$ ) and in different directions ( $X$ ,  $Y$ ,  $Z$ -directions). The stress distributions of the viscoelastic FE models under  $0.3g$  base excitation at different frequencies ( $0$ ,  $6.937$ ,  $20.00$ ,  $30.01$ ,  $39.33$  and  $50$  Hz) in  $X$ -direction,  $Y$ -direction and  $Z$ -direction were also presented as Fig. 9.

#### 4. Discussion

In this current study, a 3D idealized model was developed to investigate the vibrational responses of a spreading bone cell. Firstly, the natural frequency (resonance frequency) of the viscoelastic FE model was extracted. Then, harmonic vibration responses (displacement, stress and strain of centre of nucleus) of the viscoelastic FE models were analysed for the different base excitation acceleration values ( $0.15g$ ,  $0.3g$  and  $0.5g$ ).

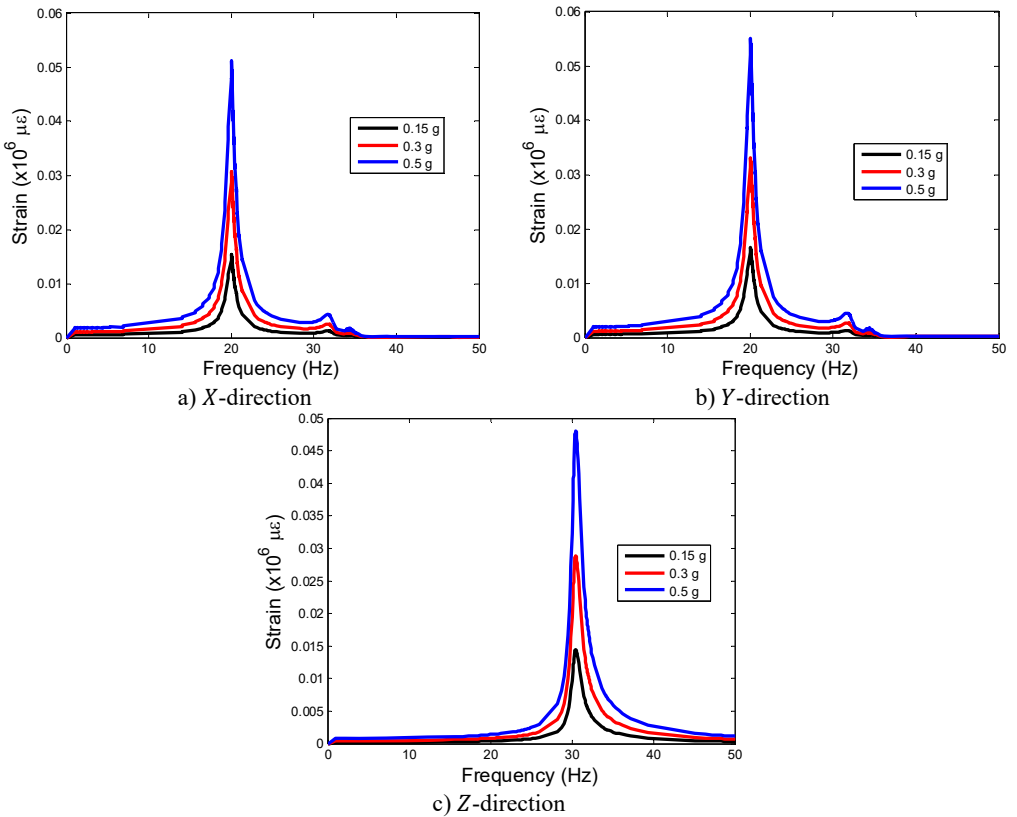


Fig. 6. The strain values of the centre of nucleus versus frequency under the different acceleration values

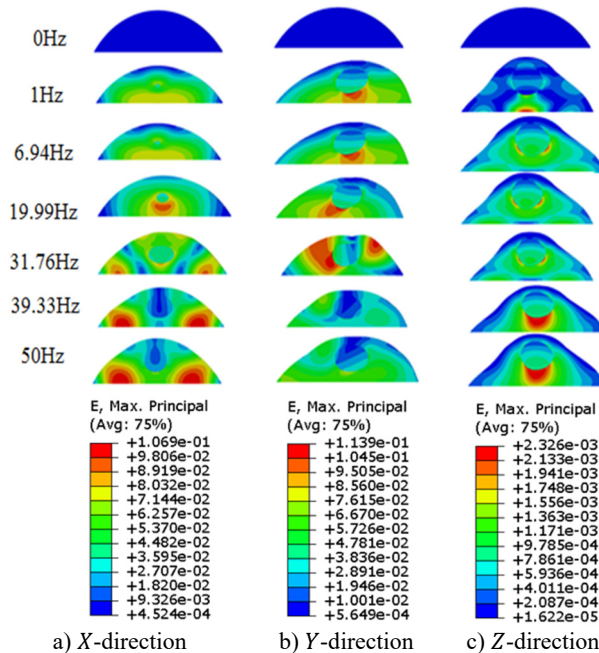
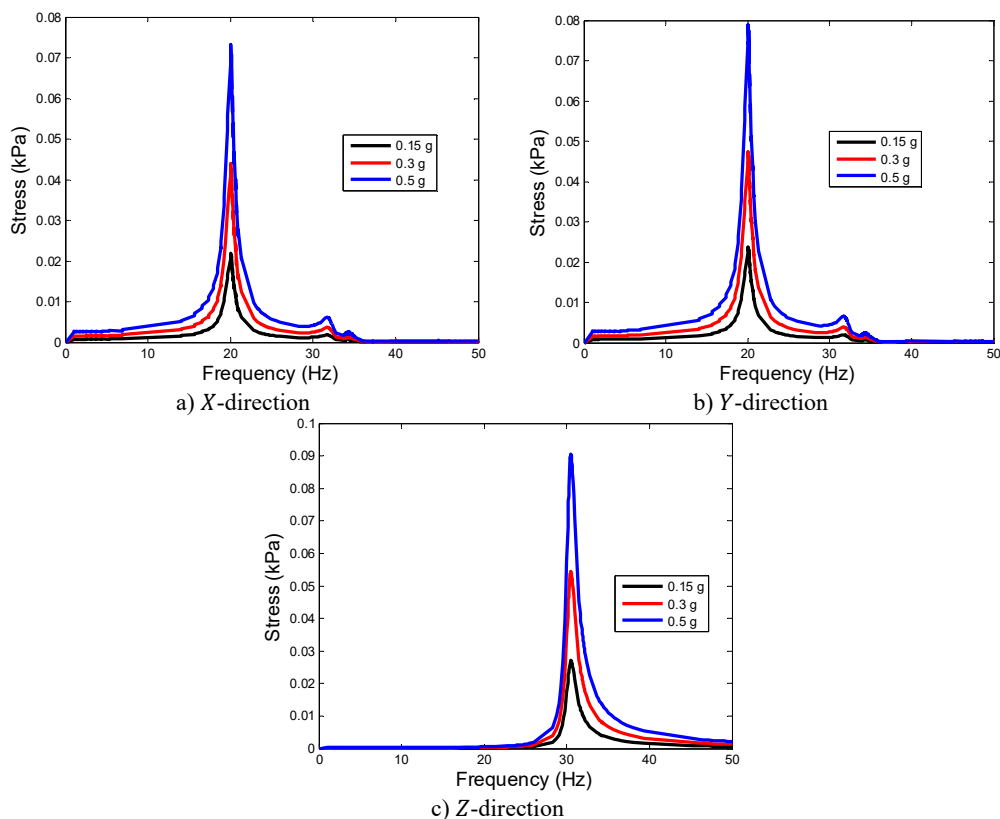


Fig. 7. Strain contours of the cell under 0.3g acceleration for different frequencies and in X-direction, Y-direction and Z-direction

The natural frequency of a bone cell (osteoblast) was predicted by using the viscoelastic FE model, with the first ten resonant frequencies of the cell being found between 19.99-34.48 Hz (Fig. 3). Based on the previous in vitro experimental studies, the vibration frequencies (5-100 Hz) were selected for the bone cell [9, 45]. The vibration frequency is important for bone cells to complete the bone bone formation and bone resorption [2, 46]. Similar natural frequency values were computed by other FE studies, e.g. the first ten natural frequencies an osteoblast were predicted as ~9.95-211.05 Hz [26] and as ~18.11-21.05 Hz [27]. Compared with the previous studies, it can be found that first ten natural frequencies from the current viscoelastic FE model are within the ranges from the literature. Therefore, the current viscoelastic FE model can be used to analyse the vibration behaviours of osteoblasts. In addition, it is noted that the natural frequencies are dependent on the material properties like density and geometry like the spreading shape.



**Fig. 8.** The stress values of the centre of nucleus versus frequency under different acceleration values

It is well known that the vibration responses depend on not only the excitation frequency but also how well the excitation conditions match the natural frequency and mode shape. For human activity, the acceleration is 1 *g*, 3-4 *g* and 5 *g* for walking, running and jumping hurdles, respectively [47]. In another study, the acceleration of 0.04-19.3 *g* was used in a human vibration test, and the resonant frequencies were found to be 10-40 Hz, 10-25 Hz, 10-20 Hz and 10 Hz for ankle, knee, hip and spine, respectively [48]. In the current study, the one-degree-of-freedom vibrational system was applied, and the three different base excitation accelerations, 0.15 *g*, 0.3 *g* and 0.5 *g*, were used to investigate the effect of acceleration on the response of the bone cell. The results showed that the natural frequency does not change with the change of the base excitation acceleration, because the natural frequency of a bone cell is determined by the intrinsic factors of



the cell (such as density) and is not affected by the external factors like loading.

In the present study, the displacement, strain and stress responses of an osteoblast were predicted by using the viscoelastic FE model under different accelerations. From Figs. 4, 6 and 8, it can be seen that the value of the displacement, strain and stress increase with the increasing acceleration. It also can be found that the values in X-direction are slightly smaller than those for the Y-direction, and the values in X-direction and Y-direction are larger than those of the Z-direction for the same acceleration in the three directions. In addition, the peak frequency values in X-direction and Y-direction are similar for the 1st vibration mode and Z-direction at 4th vibration mode. Wee and Voloshin [27] found that the resonance phenomenon of the bone cell in X-direction, Y-direction and Z-direction occurred at mode 1, mode 2 and mode 3, respectively. The resonance phenomenon of the bone cell depends on the geometry of the model.

Our FE analysis suggests that strain and stress are basically concentrated around the nucleus in Z-direction and move away from the centre of nucleus with the increasing frequency for the harmonic response under the 0.3g acceleration (Figs. 7 and 9). It can be also revealed that the strain and stress distributions are different for the acceleration acting at X-direction, Y-direction and Z-direction due to the geometry and vibration direction.

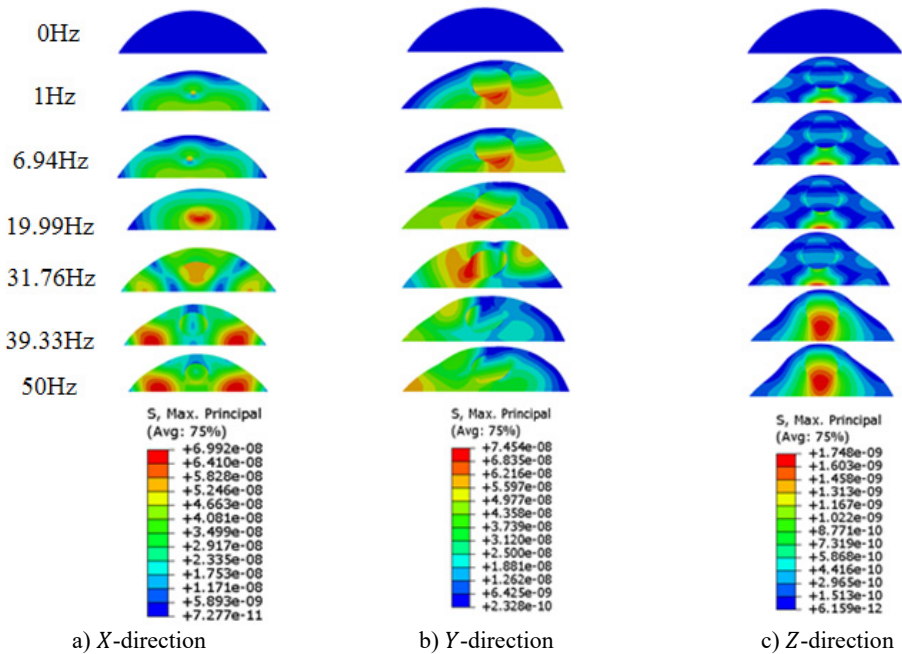


Fig. 9. Stress contours of the cell under 0.3g acceleration for different frequencies and in X-direction, Y-direction and Z-direction

## 5. Conclusion

In the current study, a viscoelastic FE osteoblast model was developed, and the natural frequencies of the osteoblast FE model were extracted and the harmonic responses were analyzed under different acceleration values (0.15g, 0.3g and 0.5g). It is found that the natural frequency range is between 19.99 and 34.48 Hz for the osteoblast FE model. The response values of displacement, strain and stress increase with the increase of base excitation acceleration. In addition, the response values in Z-direction are much bigger than those in the other directions (X, Y-direction) for the same base excitation acceleration. This osteoblast FE model could potentially be used to investigate cell deformation due to vibrational stimuli in vitro. It will help us to

understand and guide the cell culture experiments in vitro.

## Acknowledgements

This work was supported by the National Natural Science Foundation of China (81671928). LW is supported by Australian National Health and Medical Research Council (NHMRC) Postgraduate Research Scholarship Grant, and CJX is supported by the NHMRC Senior Research Fellowship.

## References

- [1] **Lim C., Zhou E., Quek S.** Mechanical models for living cells – a review. *Journal of Biomechanics*, Vol. 39, 2006, p. 195-216.
- [2] **Tirkkonen L., Halonen H., Hyttinen J., Kuokkanen H., Sievänen H., Koivisto A.-M., et al.** The effects of vibration loading on adipose stem cell number, viability and differentiation towards bone-forming cells. *Journal of The Royal Society Interface*, Vol. 8, 2011, p. 1736-1747.
- [3] **Carter D. R.** Mechanical loading history and skeletal biology. *Journal of Biomechanics*, Vol. 20, 1987, p. 1095-1109.
- [4] **Turner C. H., Forwood M., Rho J. Y., Yoshikawa T.** Mechanical loading thresholds for lamellar and woven bone formation. *Journal of Bone and Mineral Research*, Vol. 9, 1994, p. 87-97.
- [5] **Pearson O. M., Lieberman D. E.** The aging of Wolff's "law": ontogeny and responses to mechanical loading in cortical bone. *American Journal of Physical Anthropology*, Vol. 125, 2004, p. 63-99.
- [6] **Evans E.** New membrane concept applied to the analysis of fluid shear-and micropipette-deformed red blood cells. *Biophysical Journal*, Vol. 13, Issue 9, 1973, p. 941-954.
- [7] **Kapur S., Baylink D. J., Lau K.-H. W.** Fluid flow shear stress stimulates human osteoblast proliferation and differentiation through multiple interacting and competing signal transduction pathways. *Bone*, Vol. 32, 2003, p. 241-251.
- [8] **Wang L., Dong J., Xian C. J.** Strain amplification analysis of an osteocyte under static and cyclic loading: a finite element study. *BioMed Research International*, Vol. 2015, 2015.
- [9] **Bacabac R. G., Smit T. H., Van Loon J. J., Doulabi B. Z., Helder M., Klein-Nulend J.** Bone cell responses to high-frequency vibration stress: does the nucleus oscillate within the cytoplasm? *The FASEB Journal*, Vol. 20, 2006, p. 858-864.
- [10] **Mijailovich S. M., Kojic M., Zivkovic M., Fabry B., Fredberg J. J.** A finite element model of cell deformation during magnetic bead twisting. *Journal of Applied Physiology*, Vol. 93, 2002, p. 1429-1436.
- [11] **Sato M., Ohshima N., Nerem R.** Viscoelastic properties of cultured porcine aortic endothelial cells exposed to shear stress. *Journal of Biomechanics*, Vol. 29, 1996, p. 461-467.
- [12] **Qiu J., Baik A. D., Lu X. L., Hillman E. M., Zhuang Z., Dong C., et al.** A noninvasive approach to determine viscoelastic properties of an individual adherent cell under fluid flow. *Journal of Biomechanics*, Vol. 47, 2014, p. 1537-1541.
- [13] **Fabry B., Maksym G. N., Butler J. P., Glogauer M., Navajas D., Taback N. A., et al.** Time scale and other invariants of integrative mechanical behavior in living cells. *Physical Review E*, Vol. 68, 2003, p. 41914.
- [14] **Alcaraz J., Buscemi L., Grabulosa M., Trepast X., Fabry B., Farré R., et al.** Microrheology of human lung epithelial cells measured by atomic force microscopy. *Biophysical Journal*, Vol. 84, 2003, p. 2071-2079.
- [15] **Shin D., Athanasiou K.** Cytoindentation for obtaining cell biomechanical properties. *Journal of Orthopaedic Research*, Vol. 17, 1999, p. 880-890.
- [16] **Guilak F., Mow V. C.** The mechanical environment of the chondrocyte: a biphasic finite element model of cell-matrix interactions in articular cartilage. *Journal of Biomechanics*, Vol. 33, 2000, p. 1663-1673.
- [17] **Ingber D. E., Tensegrity I.** Cell structure and hierarchical systems biology. *Journal of Cell Science*, Vol. 116, 2003, p. 1157-1173.
- [18] **Kardas D., Nackenhorst U., Balzani D.** Computational model for the cell-mechanical response of the osteocyte cytoskeleton based on self-stabilizing tensegrity structures. *Biomechanics and Modeling in Mechanobiology*, Vol. 12, 2013, p. 167-183.

- [19] **Lavagnino M., Arnoczky S. P., Kepich E., Caballero O., Haut R. C.** A finite element model predicts the mechanotransduction response of tendon cells to cyclic tensile loading. *Biomechanics and Modeling in Mechanobiology*, Vol. 7, 2008, p. 405-416.
- [20] **Miller P., Hu L., Wang J.** Finite element simulation of cell–substrate decohesion by laser-induced stress waves. *Journal of the Mechanical Behavior of Biomedical Materials*, Vol. 3, 2010, p. 268-277.
- [21] **Kim E., Guilak F., Haider M. A.** The dynamic mechanical environment of the chondrocyte: a biphasic finite element model of cell-matrix interactions under cyclic compressive loading. *Journal of Biomechanical Engineering*, Vol. 130, 2008, p. 061009.
- [22] **McGarry J., Prendergast P.** A three-dimensional finite element model of an adherent eukaryotic cell. *Journal of European Cells and Materials*, Vol. 7, 2004, p. 27-33.
- [23] **Katzengold R., Shoham N., Benayahu D., Gefen A.** Simulating single cell experiments in mechanical testing of adipocytes. *Biomechanics and Modeling in Mechanobiology*, Vol. 14, 2015, p. 537-547.
- [24] **Slomka N., Gefen A.** Confocal microscopy-based three-dimensional cell-specific modeling for large deformation analyses in cellular mechanics. *Journal of Biomechanics*, Vol. 43, 2010, p. 1806-1816.
- [25] **Darling E. M., Topel M., Zauscher S., Vail T. P., Guilak F.** Viscoelastic properties of human mesenchymally-derived stem cells and primary osteoblasts, chondrocytes, and adipocytes. *Journal of Biomechanics*, Vol. 41, 2008, p. 454-464.
- [26] **Wee H., Voloshin A.** Modal analysis of a spreading osteoblast cell in culturing. 38th Annual Northeast Bioengineering Conference (NEBEC), 2012, p. 167-168.
- [27] **Wee H., Voloshin A.** Dynamic analysis of a spread cell using finite element method. *Mechanics of Biological Systems and Materials*, Vol. 4, 2014, p. 135-40.
- [28] **Zhu C., Bao G., Wang N.** Cell mechanics: mechanical response, cell adhesion, and molecular deformation. *Annual Review of Biomedical Engineering*, Vol. 2, 2000, p. 189-226.
- [29] **Guilak F., Tedrow J. R., Burgkart R.** Viscoelastic properties of the cell nucleus. *Biochemical and Biophysical Research Communications*, Vol. 269, 2000, p. 781-786.
- [30] **Costa K. D.** Single-cell elastography: probing for disease with the atomic force microscope. *Disease Markers*, Vol. 19, 2004, p. 139-154.
- [31] **Frisch T., Thoumine O.** Predicting the kinetics of cell spreading. *Journal of Biomechanics*, Vol. 35, 2002, p. 1137-1141.
- [32] **Deguchi S., Fukamachi H., Hashimoto K., Iio K., Tsujioka K.** Measurement and finite element modeling of the force balance in the vertical section of adhering vascular endothelial cells. *Journal of the Mechanical Behavior of Biomedical Materials*, Vol. 2, 2009, p. 173-185.
- [33] **Abolfathi N., Karami G., Ziejewski M.** Biomechanical cell modelling under impact loading. *International Journal of Modelling and Simulation*, Vol. 28, 2008, p. 470-476.
- [34] **Kamm R., McVittie A., Bathe M.** On the role of continuum models in mechanobiology. *ASME Applied Mechanics Division*, Vol. 242, 2000, p. 1-12.
- [35] **Milner J. S., Grol M. W., Beaucage K. L., Dixon S. J., Holdsworth D. W.** Finite-element modeling of viscoelastic cells during high-frequency cyclic strain. *Journal of Functional Biomaterials*, Vol. 3, 2012, p. 209-224.
- [36] **Vichare S., Inamdar M. M., Sen S.** Influence of cell spreading and contractility on stiffness measurements using AFM. *Soft Matter*, Vol. 8, 2012, p. 10464-10471.
- [37] **Ronan W., Deshpande V. S., McMeeking R. M., McGarry J. P.** Numerical investigation of the active role of the actin cytoskeleton in the compression resistance of cells. *Journal of the Mechanical Behavior of Biomedical Materials*, Vol. 14, 2012, p. 143-157.
- [38] **Bursa J., Fuis V.** Finite element simulation of mechanical tests of individual cells. *World Congress on Medical Physics and Biomedical Engineering*, 2009, Munich, Germany, 2010, p. 16-19.
- [39] **ABAQUS V. 6.14** Documentation. Dassault Systemes Simulia Corp., Providence, RI, USA. 2014.
- [40] **Uzer G., Pongkitwiton S., Ian C., Thompson W. R., Rubin J., Chan M. E., et al.** Gap junctional communication in osteocytes is amplified by low intensity vibrations in vitro. *PloS One*, Vol. 9, Issue 3, 2014.
- [41] **McGarry J. G., Klein-Nulend J., Mullender M. G., Prendergast P. J.** A comparison of strain and fluid shear stress in stimulating bone cell responses – a computational and experimental study. *The FASEB Journal*, Vol. 19, 2005, p. 482-484.
- [42] **Ferko M. C., Bhatnagar A., Garcia M. B., Butler P. J.** Finite-element stress analysis of a multicomponent model of sheared and focally-adhered endothelial cells. *Annals of Biomedical Engineering*, Vol. 35, 2007, p. 208-223.

- [43] **Beck B. R.** Vibration therapy to prevent bone loss and falls: mechanisms and efficacy. *Current Osteoporosis Reports*, Vol. 13, 2015, p. 381-389.
- [44] **Nagaraja M. P., Jo H.** The role of mechanical stimulation in recovery of bone loss – high versus low magnitude and frequency of force. *Life*, Vol. 4, 2014, p. 117-130.
- [45] **Rosenberg N., Levy M., Francis M.** Experimental model for stimulation of cultured human osteoblast-like cells by high frequency vibration. *Cytotechnology*, Vol. 39, 2002, p. 125-130.
- [46] **Lau E., Al-Dujaili S., Guenther A., Liu D., Wang L., You L.** Effect of low-magnitude, high-frequency vibration on osteocytes in the regulation of osteoclasts. *Bone*, Vol. 46, 2010, p. 1508-1515.
- [47] **Marcus R.** Exercise: moving in the right direction. *Journal of Bone and Mineral Research*, Vol. 13, 1998, p. 1793-1796.
- [48] **Kiiski J., Heinonen A., Järvinen T. L., Kannus P., Sievänen H.** Transmission of vertical whole body vibration to the human body. *Journal of Bone and Mineral Research*, Vol. 23, 2008, p. 1318-1325.



**Liping Wang** received B.Eng. degree in mechanical engineering from Beihang University, Beijing, China, in 1996 and M.Eng. degree in mechanical engineering from Tianjin University, Tianjin, China, in 2005. She now works at the University of South Australia, Adelaide, Australia. Her research interests include mechanical design, mechanical processing, reverse engineering, biomechanics and biomaterials.



**Cory J. Xian** obtained his Ph.D. in 1993 from Murdoch University (Perth, Australia). He has been interested in research into tissue growth, injury repair and roles of growth factors/cytokines and progenitor cells. Currently, he is a research Professor at University of South Australia (Adelaide, Australia) leading research on bone growth, injury repair, regeneration, and cancer chemotherapy-induced bone defects.